Hydrophobic Anion Activation of Human Liver χχ Alcohol Dehydrogenase†

Jean-Marc Moulis,‡,§ Barton Holmquist, and Bert L. Vallee*

Center for Biochemical and Biophysical Sciences and Medicine and Department of Biological Chemistry and Molecular Pharmacology, Harvard Medical School, 250 Longwood Avenue, Boston, Massachusetts 02115

Received November 27, 1990; Revised Manuscript Received March 12, 1991

ABSTRACT: Class III alcohol dehydrogenase (χχ-ADH) from human liver binds both ethanol and acetaldehyde so poorly that their K_m values cannot be determined, even at ethanol concentrations up to 3 M. However, long-chain carboxylates, e.g., pentanoate, octanoate, deoxycholate, and other anions, substantially enhance the binding of ethanol and other substrates and hence the activity of class III ADH up to 30-fold. Thus, in the presence of 1 mM octanoate, ethanol displays Michaelis–Menten kinetics. The degree of activation depends on the size both of the substrate and of the activator; generally, longer, negatively charged activators result in greater activation. At pH 10, the activator binds to the E–NAD^+ form of the enzyme to potentiate substrate binding. Pentanoate activates methylcrotyl alcohol oxidation and methylcrotyl aldehyde reduction 14- and 30-fold, respectively. Such enhancements of both oxidation and reduction are specific for class III ADH; neither class I nor class II shows this effect. The implications as to the nature of the physiological substrate(s) of class III ADH are discussed in light of the recent finding that this ADH and glutathione-dependent formaldehyde dehydrogenase are identical. A new rapid purification procedure for χχ-ADH is presented.

Ethanol oxidation in man occurs primarily in the liver, which contains three classes of alcohol dehydrogenase (ADH).[1] The isozymes of class I, together with class II, are most abundant, and, compared with class III, their activities toward ethanol are much higher and, hence, are most likely responsible for its oxidation. Following oral ingestion ethanol is rapidly distributed throughout the body and freely passes the blood/brain, testicular, and placental barriers. All of these organs are incapable of removing ethanol since they only contain class III ADH, which hardly oxidizes ethanol at all.

First isolated from human placenta where it is the only ADH present (Parês & Vallee, 1981), χχ-ADH is also the only ADH isozyme in brain (Beisswenger et al., 1985). It also predominates in testis (Dafeldecker & Vallee, 1986) and is now known to be present in nearly all tissues. The enzyme is homologous with all other human ADH isozymes (Kaiser et al., 1988) and is composed of two identical 40 000-dalton subunits forming a homodimer which contains 4 mol of zinc. Its isoelectric point, 6.4, is low compared to that of the other ADH classes and isozymes (Wagner et al., 1984). In spite of its similarity with all of these, the catalytic behavior of χχ-ADH toward ethanol differs significantly: the K_m of χχ-ADH toward this substrate cannot be measured at concentrations up to 3 M. This is in sharp contrast with the values observed for all human class I and II enzymes as well as the corresponding forms of the horse enzyme (Wagner et al., 1983; Eklund et al., 1990). Yet, when presented with long-chain hydrophobic primary alcohols, the enzyme is nearly as effective a catalyst as the class I forms (Wagner et al., 1984).

The low activity of χχ-ADH toward ethanol has been attributed to specific substitutions in its substrate binding domain (Juliá et al., 1988; Kaiser et al., 1989). Compared to class I, its volume is markedly greater due to substitutions with smaller and more hydrophilic residues. This additional space and greater hydrophilicity of the substrate pocket allow the accommodation and binding of more water which may only be displaced by longer and more hydrophobic substrates. Ethanol is thought to be incapable of displacing the water, accounting for its poor activity (Eklund et al., 1989). However, the findings presented here suggest that binding of an anionic hydrophobic ligand to χχ-ADH can potentiate both the oxidation of ethanol and that of other alcohols, serving a regulatory mechanism which controls alcohol and/or aldehyde metabolism. Octanoic acid, in fact, potentiates ethanol binding to such an extent that a K_m can be measured.

Recently, the sequences of peptides from rat glutathione-dependent formaldehyde dehydrogenase (Koivusalo et al., 1989) have been found identical with the sequence of class III ADH (Kaiser et al., 1988), and on this basis, the two enzymes are thought to be the same (Koivusalo et al., 1989). Formaldehyde dehydrogenase has been purified from various sources, among them human liver (Uotila & Koivusalo, 1974), and shown to catalyze the oxidation of *S*-(hydroxymethyl)-glutathione to *S*-formylglutathione, a reaction chemically equivalent to those catalyzed by ADH. The nature of the physiological substrate for this enzyme remains to be established, and we have continued to investigate the catalytic behavior of class III ADH toward alcohol substrates. We present evidence here for the activation of alcohol oxidation and aldehyde reduction by long-chain anions. The characteristics of this process and some aspects of its mechanism are described.

Materials and Methods

Materials. Pentanol, pentanal, and 3-methylcrotyl alcohol were distilled before use. 3-Methyl-2-butenoic acid (Pfaltz and Bauer, Waterbury, CT) was recrystallized from diethyl ether saturated with water to give white needles, which were dried extensively under vacuum. 5β-Cholan-3α,7α,12α,24-

† This work was supported by a grant from the Samuel Bronfman Foundation, with funds provided by Joseph E. Seagram and Sons, Inc.

‡ Present address: DBMS/Métalloprotéines, CENG 85X, 38041 Grenoble Cedex, France.

§ Supported in part by the Foundation pour la Recherche Medicale.

[1] Abbreviations: ADH, alcohol dehydrogenase; DEAE, diethylaminoethyl; Tris, tris(hydroxymethyl)aminomethane; DTT, dithiothreitol; AG–AMP, agarose–hexane–adenosine 5′-phosphate affinity resin; MCA, 3-methyl-2-butene-1-ol (methylcrotyl alcohol); CA, *N*-[1(5)carboxy-5-aminopentyl]; Cbz, carbobenzoxy; SDS, sodium dodecyl sulfate; Boc, *N*-*tert*-butoxycarbonyl; HPLC, high-performance liquid chromatography.

0006-2960/91/0430-5743$02.50/0

tetrol (Steraloids Inc., Wilton, NH) was recrystallized from ethanol–water and dried under vacuum. Buffers and cofactors (NAD^+, grade III, and NADH), phosphatidic acids, phosphatidylserine, and phosphoinositides were obtained from Sigma. All other chemicals were the best grade available.

Enzyme Assays. ADH activity and initial velocity measurements were made with a Cary 219 or a Gilford 2600 spectrophotometer following the appearance (alcohol oxidation) or disappearance (aldehyde reduction) of NADH at 340 nm and 25 °C as described (Wagner et al., 1984).

Velocity–substrate concentration data pairs used to determine kinetic constants were stored and fitted to the Michaelis–Menten equation using an Apple II computer with software provided by Varian Associates, Palo Alto, CA. The reported two-substrate data produced linear primary and secondary plots that intersect and were analyzed by least-squares iteration (Cleland, 1967) using the sequential bi-bi model according to

$$v = [E]k_{cat}/\left[1 + \frac{K_m^{NAD}}{[NAD]} + \frac{K_m^{Alc}}{[Alc]} + \frac{K_m^{Alc}K_s^{NAD}}{[NAD][Alc]}\right]$$

Kinetic experiments involving very hydrophobic compounds were carried out in the presence of up to 5% (v/v) methanol, where indicated. This alcohol is not oxidized by χχ-ADH nor is it inhibitory at these concentration (Parés & Vallee, 1981). The steady-state kinetic parameters for octanol in the presence and absence of 2% (v/v) methanol were identical.

Experiments with arachidonate were carried out under nitrogen. Buffer and substrate solutions were thoroughly saturated with nitrogen before use, and rates were measured in stoppered cuvettes.

Starch gel electrophoresis was performed according to Wagner et al. (1983) and SDS–polyacrylamide gel electrophoresis by the method of Laemmli and Favre (1973).

Purification of Class III ADH. Throughout purification, class III ADH activity was measured by using 0.5 mM ω-hydroxydodecanoic acid as substrate in 0.1 M glycine–NaOH buffer, pH 10.0, 20 mM NaCl, 2.5 mM NAD^+, and 2 mM 4-methylpyrazole. The presence of the large amount of 4-methylpyrazole, a class I ADH inhibitor, allows the detection of class III ADH activity in mixtures containing various amounts of other ADH isozymes. This assay proved more reliable at all stages of the purification scheme than the one using 0.5 M ethanol as substrate (Wagner et al., 1984). Unless otherwise stated, all purification steps were done at 4 °C. The enzymes were isolated from adult human livers, obtained at autopsy and stored at −70 °C, by a modification of a published procedure (Wagner et al., 1984) as follows.

Human liver (100 g) was cut into pieces (approximately 4 × 4 cm) and thawed in 100 mL of distilled water containing 1 mM sodium ascorbate. The tissue was ground in a Waring blender and then homogenized in a Polytron (Brinkmann Instruments, Westbury, NY) homogenizer. The homogenate was centrifuged immediately for 45 min at 20000*g*. The supernatant was dialyzed overnight against 15 L of 10 mM Tris-HCl buffer, pH 7.9, containing 1 mM sodium ascorbate.

The dialyzed homogenate was then passed through 500 mL of DEAE-cellulose (DE-52, Whatman International Ltd., Maidstone, England) equilibrated with 10 mM Tris-HCl buffer, pH 7.9, containing 1 mM sodium ascorbate and packed in a sintered glass funnel. Class I and II isozymes were washed from the resin with the equilibration buffer and purified further (Wagner et al., 1983; Ditlow et al., 1984). The bound χχ-ADH was then eluted with 500 mL of 0.1 M Tris-HCl–0.5 M NaCl containing 1 mM ascorbate, pH 8. Octanal, from a 10 mM solution in methanol, was added to the pooled eluate to a concentration of 10 μM and the fraction concentrated to about 100 mL with an Amicon concentrator (Danvers, MA) equipped with a PM 30 membrane. The concentrated enzyme solution was dialyzed against 15 L of 50 mM sodium phosphate buffer, pH 7.4, and 1 mM sodium ascorbate and then against the same buffer but with 0.5 mM DTT instead of ascorbate.

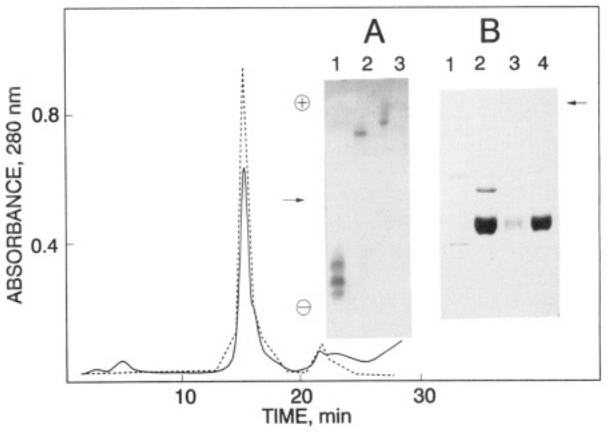

FIGURE 1: HPLC chromatography of class III ADH isozymes. Approximately 3 mg of protein (0.35 mL) from the AG–AMP affinity column in 10 mM Tris-HCl and 1 mM DTT, pH 8.0, was loaded on the 7.5 cm × 7.5 mm HPLC DEAE 5PW column equilibrated with the same buffer. The column was developed at a flow rate of 1 mL/min with a NaCl gradient with linear segments in the same buffer with the following program: time (min), [NaCl] (mM): 0, 0; 5, 20; 12, 24; 15, 40; 20, 40; 25, 200. The absorbance at 280 nm was monitored (—), and 0.5-mL fractions were collected and assayed for activity (– – –) as described under Materials and Methods. Inset: Electrophoresis of purified human class III ADH. (A) Starch gel electrophoresis: (lane 1) crude extract; (lane 2) χχ-ADH, 14.5-min peak; (lane 3) $\chi_2\chi_2$-ADH, 21.3-min peak. The gel was stained for ADH activity with pentanol as substrate. (B) SDS–polyacrylamide gel electrophoresis: (lane 1) molecular weight standards, bovine serum albumin (67K), ovalbumin (46K), and carbonic anhydrase (29K); (lane 2) χχ-ADH fraction from the AMP column; (lane 3) 5.5 μg of HPLC-purified χχ-ADH; (lane 4) 10 μg of HPLC-purified $\chi_2\chi_2$-ADH. Coomassie Blue R-250 was used to stain the gel.

For all the following steps, the sodium ascorbate antioxidant was replaced by 0.1 mM DTT in all buffers. The dialyzed solution was clarified by centrifugation for 20 min at 20000*g* and loaded onto a 1.5 × 5 cm column of AG–AMP type 2 (P-L Biochemicals, Milwaukee, WI) equilibrated with 50 mM sodium phosphate buffer, pH 7.4, at a flow rate of approximately 1 column volume/h. The column was then washed extensively with the equilibration buffer and developed with a total of 200 mL of a 0–25 μM NADH linear gradient prepared in 10 mM Tris-HCl, pH 8.0. The active fractions eluted at 2–3 μM NADH and were pooled and concentrated by use of an Amicon concentrator with a PM 30 membrane, after making the solution 10 μM in octanal. The enzyme solution was repeatedly concentrated and diluted with 10 mM Tris-HCl, pH 8.0, until no NADH absorbance at 340 nm remained in the effluent (usually after 5 × 1:10 dilutions).

The final purification step was performed at ambient temperature with a DEAE 5PW (Waters, Milford, MA) anion-exchange HPLC column equilibrated with 10 mM Tris-HCl, pH 8.0, and eluted with a NaCl gradient (Figure 1). About 80% of the activity was recovered in a major peak with a retention time of 14.5 min and a minor peak appearing at 21.3 min. The second peak corresponds to a second form of class III ADH ($\chi_2\chi_2$-ADH) that migrates on starch gel electrophoresis more anodically than the major (χχ-ADH) enzyme (Parés & Vallee, 1981; Vallee & Bazzone, 1983; Adinolfi et

Table I: Purification of Human Liver Class III ADH (per 100 g of Tissue)

fraction	vol (mL)	protein concn[a] (mg/mL)	total units[b]	yield (%)	sp act (units/mg)	n-fold purification
crude extract	150	33	29.1	100	0.006	1
DEAE column	500	3.9	18.6	64	0.01	1.6
AG-AMP column	12.5	2.4	14.6	50	0.49	83
HPLC	2.2	3.9	10.8[c]	37	1.25	210

[a] Determined by the method of Lowry (1951) with bovine serum albumin as standard. [b] Measured with 0.5 mM 12-hydroxydodecanoic acid as substrate, 0.1 M glycine, 20 mM NaCl, 2 mM 4-methylpyrazole, and 2.4 mM NAD^+ at pH 10.0. [c] 4-Methylpyrazole omitted from the assay. Only the activity of the first peak eluting at 14.5 min (see Results) is considered here.

al., 1984; Valkonen & Goldman, 1988). The active fractions were separately concentrated with Centricon 30 microconcentrators (Amicon) and kept as beads in liquid nitrogen. A summary of the purification is shown in Table I. This improved procedure was also used to isolate horse χχ-ADH (Dafeldecker & Vallee, 1982). It eluted from the HPLC column 7 min later that the human χχ-ADH under identical conditions.

Results

Enzyme Purification. With the present purification of χχ-ADH, highly purified enzyme can be obtained in only 3–4 days (Table I), a significant improvement considering its lability (Wagner et al., 1984). The resultant enzyme is stable for at least 1 year without loss in specific activity when stored in liquid nitrogen.

The chromatography on an anion-exchange HPLC column in the final step is the primary improvement in the purification process. χχ-ADH is the major active fraction which appears from the HPLC column at 14.5 min; it is completely homogeneous, as indicated by starch and SDS–polyacrylamide gel electrophoresis (Figure 1). A second active peak is also resolved; it presumably corresponds to the form of the enzyme ($\chi_2\chi_2$-ADH) reported earlier (Parés & Vallee, 1981; Adinolfi et al., 1984; Valkonen & Goldman, 1988), and has been shown to have an identical sequence with χχ-ADH (Kaiser et al., 1991).

Catalytic Properties. Previous studies (Parés & Vallee, 1981; Wagner et al., 1984; Beisswenger et al., 1985) have demonstrated that ethanol is a poor substrate for χχ-ADH and methanol is not a substrate at all. The K_m and k_{cat} values determined by Lineweaver–Burk analysis of a more extensive substrate specificity survey demonstrate that an increase of the aliphatic chain of primary alcohols decreases the apparent Michaelis constant (Table II). However, the k_{cat} values of *n*-alkanols with chains longer than *n*-octanol also decrease progressively; the catalytic efficiency, as judged by k_{cat}/K_m, remains nearly constant. The most active alcohol thus far is 3,7,11-trimethyl-2,6,10-dodecatrien-1-ol (farnesol) (k_{cat}/K_m = 3700 mM^{-1} min^{-1}), which in addition to its long aliphatic chain contains the 2-alkene bond. Its k_{cat}, 220 min^{-1}, is close to the highest value yet observed for any ADH substrate. The k_{cat} values for 3-methyl-2-buten-1-ol (MCA) and cinnamyl alcohol are also high; like farnesol, they too contain the 3-substituted 2-alkene-1-ol unit.

Class III ADH can also very effectively oxidize *S*-(hydroxymethyl)glutathione, the hemithiol acetal formed between glutathione and formaldehyde (Koivusalo et al., 1989), but it is completely inactive toward methanol up to 5 M. The presence of a nucleophilic species (alkene or sulfur) on the atom adjacent to the carbon to which the hydroxyl is bound apparently greatly enhances catalysis.

Activation of χχ-ADH Ethanol Activity. Increasing concentrations of various carboxylic acids instantaneously enhance χχ-ADH-catalyzed ethanol oxidation to a degree and with a concentration dependence that varies with the structure of the activating acid (Figure 2). When ethanol is the substrate ([S] ≪ K_m), an increase in activity of up to 3.4-fold can be reached at pH 10. Deoxycholate near 1 mM induces this degree of maximal activation. With octanoate or cinnamate, this extent of activation is observed only above 2 mM. Both arachidonate and SDS double the χχ-ADH activity at concentrations as low as 100 μM but inhibit at higher concentrations, presumably due to subunit dissociation in the case of SDS.

At concentrations higher than 10 mM, chloride and nitrate increase the rate of 0.5 M ethanol oxidation by a factor of about 1.4, but bromide, carbonate, and sulfate have little effect. Significant activation seems limited to anionic hydrophobic agents without additional hydrophilic substituents. Thus, citrate and succinate, phospholipids including phosphatidic

Table II: Substrate Specificity of Human Liver χχ-ADH[a]

alcohol	K_m (mM)	k_{cat} (min^{-1})[d]	k_{cat}/K_m (mM^{-1} min^{-1})
n-pentanol	24.3	174	7
n-hexanol	8.2	31	16
n-octanol	1.2	223	185
n-nonanol[b]	0.27	53	201
n-decanol[b]	0.18	40	150
n-dodecanol[b]	0.05	18	310
n-tetradecanol[b]	0.006	1	160
cis-2-hexene-1-ol	2.9	228	78
trans-2-hexene-1-ol	0.9	244	272
3-methyl-2-butene-1-ol	14.6	320	22
farnesol[c]	0.06	220	3700
2-butene-1,4-diol	46	230	5
1,6-hexanediol	12	154	13
1,8-octanediol	5.5	201	37
benzyl alcohol	170	315	2
cinnamyl alcohol	0.44	163	368
5β-cholan-3α,7α,12α,24-tetrol[b]	0.2	55	279
12-hydroxydodecanoate	0.06	167	2820
GSH–formaldehyde[e]	0.004	200	50000

[a] Measured in 0.1 M glycine, 20 mM NaCl, and 2.5 mM NAD^+ at pH 10.0. [b] Assays contained 2% methanol. [c] Assays contained 5% methanol. [d] Based on a molecular weight of 80000 (Wagner et al., 1984). [e] 1 mM GSH, 1 mM formaldehyde, 50 mM sodium phosphate, and 1.25 mM NAD^+, pH 8.0.

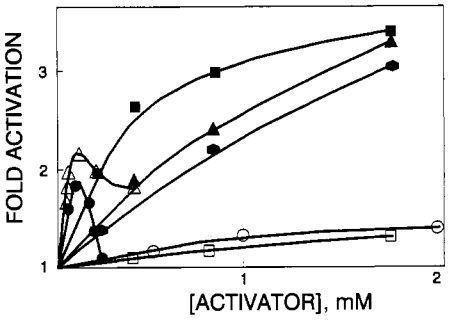

FIGURE 2: Effect of hydrophobic anions on ethanol oxidation by χχ-ADH at pH 10 in 0.1 M glycine, 2.5 mM NAD^+, and 20 mM NaCl with 0.5 M ethanol as substrate. Deoxycholate (▲), octanoate (■), cinnamate (●), octanesulfonate (○), pentanoate (□), arachidonate (△), and sodium dodecyl sulfate (●). Assay solutions of arachidonic acid contained 2% methanol.

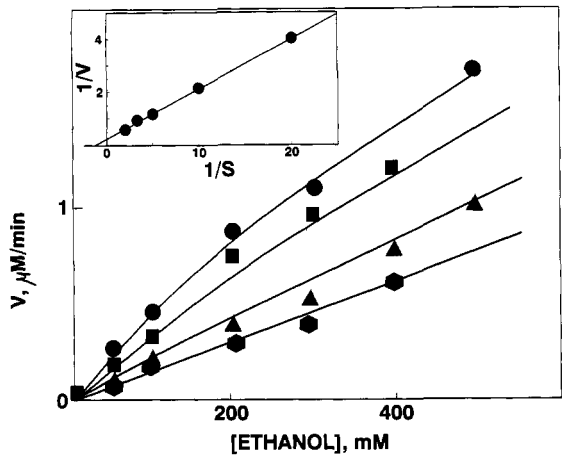

FIGURE 3: v vs [S] plots for ethanol oxidation by χχ-ADH in the absence and presence of octanoate at pH 10 in 0.1 M glycine: (●) none; (▲) 0.1; (■) 0.5; (●) 1 mM. Insert: Lineweaver–Burk plot for 1 mM octanoate.

acids, phosphatidylserine and phosphoinositides, various peptides, e.g., Boc-CA-Phe and Cbz-CA-Gly-Phe, and valeramide and valeric acid ethyl ester all fail to activate ethanol oxidation by the enzyme.

Initial velocity studies as a function of ethanol concentration indicate that, in the absence of activator, ethanol does not saturate χχ-ADH and a K_m cannot be measured (Figure 3), as reported previously (Parês & Vallee, 1981; Wagner et al., 1984). However, octanoate increases activity, and at 1 mM, an apparent K_m of 1.3 M for ethanol can be estimated (Figure 3, insert), but in the absence of ethanol, χχ-ADH together with these acids neither reduces NAD^+ nor oxidizes NADH.

Other human ADH isozymes are not activated in this manner. Octanoic acid, either 1 or 0.2 mM, does not affect the activity of $\alpha\beta_1$, $\alpha\gamma_1$, $\beta_1\beta_1$, $\beta\gamma_1$, and $\beta\gamma_2$ (class I) or of class II ADH toward 33 mM ethanol (2.4 mM NAD^+, pH 10, and 0.1 M glycine). Since the activation of χχ-ADH activity toward ethanol is measured under conditions where [S] $\ll K_m$, the activation of $\alpha\beta_1$, $\beta_1\beta_1$, $\beta\gamma_1$, and $\alpha\gamma_1$ was also examined as above but with 100 μM ethanol as the substrate, [S] = $0.1K_m$. Again, there was no activation, but 1 mM octanoate inhibits up to 30%.

Activation of the Oxidation of Other Alcohols. The activation of class III ADH is substrate-dependent. Thus, while octanoate enhances the oxidation of ethanol (Figure 3), it inhibits that of octanol with a K_i of about 2 mM, i.e., a value approximately equal to the K_m of octanol (Table II). Hence, the activation of other, longer chain alcohols as a function of activator concentration was examined. Pentanoate optimally activates pentanol oxidation 3.2-fold, longer acids causing inhibition and shorter resulting in lesser degrees of activation. This same pattern holds for the five-carbon methylcrotyl alcohol for which pentanoate and butyrate activate up to 12-fold (Figure 4). With heptanol, a yet longer substrate, only acetate activates (2-fold) and only at relatively high concentrations (0.4 M); butyrate has no apparent effect, and pentanoate and hexanoate inhibit. The inability of class III ADH to oxidize methanol is maintained, irrespective of the presence of hydrophobic anions. Further, these activators are not particularly effective in activating the (hydroxymethyl)glutathione dehydrogenase activity of class III ADH, an observation currently under study.

The activation curve of horse liver χχ-ADH is identical with that of the human enzyme both when methylcrotyl alcohol, pH 8.5, and when ethanol, pH 10.0, are the substrates and pentanoate and octanoate are the activators, respectively.

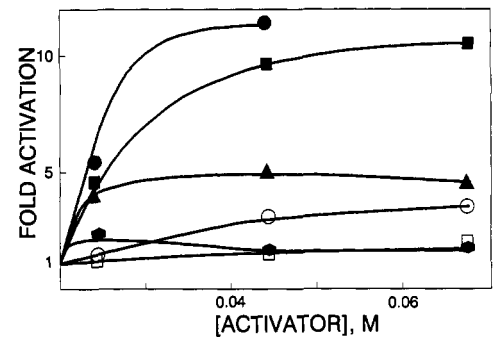

FIGURE 4: Dependence of the activity of χχ-ADH on activator concentration. Activity toward methylcrotyl alcohol measured at pH 8.5 in 50 mM phosphate. The activators are (□) acetate, (○) propionate, (■) butyrate; (●) pentanoate, (▲) hexanoate, and (●) decanoate.

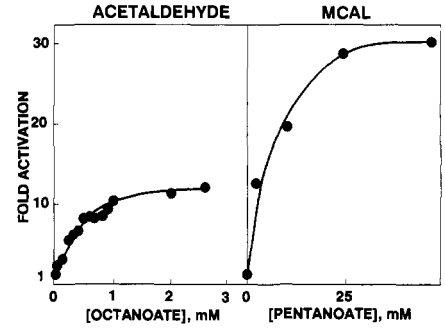

FIGURE 5: Effect of pentanoate and octanoate on the χχ-ADH-catalyzed reduction of aldehydes. Left: Effect of octanoate on acetaldehyde, 55 mM, at pH 7.0 in 50 mM Tes buffer. Right: Effect of pentanoate on methylcrotyl aldehyde (MCAL) at pH 7.5 in 50 mM phosphate and 230 μM NADH.

Activation of Aldehyde Reduction. Acetaldehyde and 3-methyl-2-buten-1-al (MCAL) reduction are both activated by octanoate and pentanoate, respectively (Figure 5). When [S] $\ll K_m$, octanoate activates acetaldehyde reduction 11-fold with half-maximal activation at 0.25 mM octanoate, while pentanoate activates methylcrotyl aldehyde 30-fold, with half-maximal activation occurring at 5 mM. This is the highest extent of activation yet observed.

Enzyme Steady-State Kinetic Parameters. To assess the influence of hydrophobic anions on the function of class III ADH, steady-state kinetic studies were carried out. In the absence of activators, the individual kinetic parameters for ethanol or acetaldehyde cannot be determined (see above). Hence, those of pentanol and methylcrotyl alcohol oxidation were examined in detail, and the effects of the respective activators 3-methyl-2-butenoate and pentanoate on these parameters were determined (Figure 6, Figure 8, and Table III). The substrate dependence of the Michaelis constant for NAD^+ indicates that the enzyme does not strictly obey an ordered Theorell and Chance kinetic mechanism (Theorell & Chance, 1951). Product inhibition studies are consistent with this conclusion (data not shown): NADH competes with pentanol at both saturating (1 mM) and nonsaturating (0.05 mM) concentrations of NAD^+ and is a mixed-type inhibitor of NAD^+ at 100 mM pentanol. In the presence of 50 mM 3-methyl-2-butenoate, the same product inhibition patterns are observed, indicating that the mechanism of alcohol oxidation at pH 10 allows some degree of randomness in the binding of cofactor and substrate, regardless of the presence of the activator.

pH Dependence of the Activation. To determine if the activation alters kinetically important ionizations, the pH

Table III: Kinetic Parameters for Alcohol Oxidation by χχ-ADH[a]

substrate	[activator] (mM)	K_m^{NAD} (μM)	K_m^{Alc} (mM)	K_s^{NAD} (μM)	k_{cat} (min^{-1})
		Pentanoate			
MCA	0	37 ± 4[c]	5.8 ± 0.8	200 ± 30	380 ± 30
	20	38 ± 8	2.0 ± 0.5	146 ± 55	350 ± 20
		3-Methyl-2-butenoate			
pentanol, pH 10	0	87 ± 11[c]	27 ± 3	118 ± 15	215 ± 13
	20	92 ± 16	15 ± 3	132 ± 35	237 ± 17
	50	95 ± 7	11 ± 2	160 ± 15	210 ± 10
	100	94 ± 20	8 ± 2	325 ± 60	234 ± 20
pentanol,[b] pH 9	0	230 ± 50	100 ± 20	60 ± 10	230 ● 30
	50	142 ± 15	20 ± 3	118 ± 15	152 ± 6

[a] Measured in 0.1 M glycine, 0.1 M Tris, and 0.2 M NaCl at pH 10. The kinetic parameters were obtained by fitting the data to a sequential bi-bi model (see Materials and Methods). [b] Same buffer as in *a*, pH 9. [c] Standard deviation from fitting to the kinetic model.

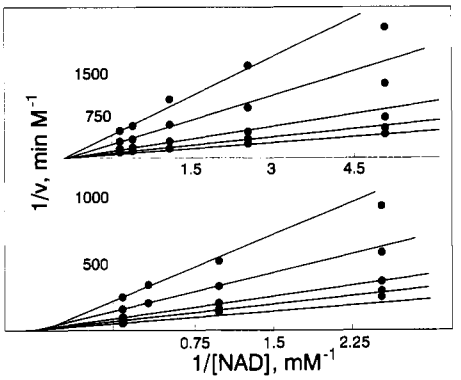

FIGURE 6: Primary Lineweaver-Burk plots for pentanol oxidation by χχ-ADH measured in 0.1 M glycine and 0.1 M Tris containing 0.2 M NaCl at pH 10.0. Top panel: no 3-methyl-2-butenoate added. Bottom panel: 50 mM 3-methyl-2-butenoate.

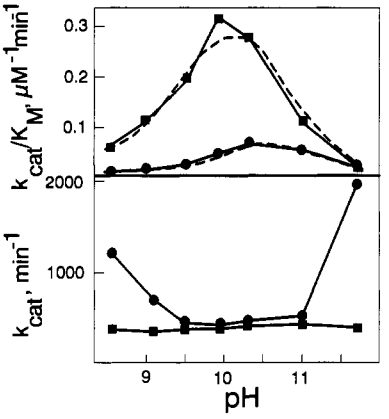

FIGURE 7: pH dependence of the kinetic parameters for methylcrotyl alcohol oxidation by χχ-ADH in the absence (●) and presence (■) of 50 mM pentanoate. The plotted parameters were obtained by fitting the data recorded from substrate concentrations spanning the apparent Michaelis constant at each pH to the Michaelis–Menten equation. The k_{cat}/K_m data were fit (---) by least squares to $y = (k_{cat}/K_m)/(1 + 10^{pK_1-pH} + 10^{pH-pK_2})$ and gave $pK_1 = 9.9$ and 9.9, $pK_2 = 11.2$ and 10.1, and $k_{cat}/K_m = 80000$ and 800000 M^{-1} min^{-1} for the curves in the absence and presence of 50 mM pentanoate, respectively. The assays were carried out in 0.1 M Tris, 0.1 M glycine, 0.5 M NaCl, and 2.5 mM NAD$^+$ at the required pH.

dependence of the individual kinetic constants of MCA oxidation in the absence and presence of 50 mM pentanoate was determined. At pH 9 as compared to pH 10, in the absence of activator the Michaelis constants for pentanol and NAD$^+$ are increased while K_s^{NAD} is decreased (Table III). At pH 9, the activator modifies K_m^{Alc} and K_s^{NAD} as at pH 10, but also decreases K_m^{NAD} and k_{cat} (Table III). The pH profiles of the kinetic constants of methylcrotyl alcohol oxidation with and without 50 mM pentanoate were determined at saturating

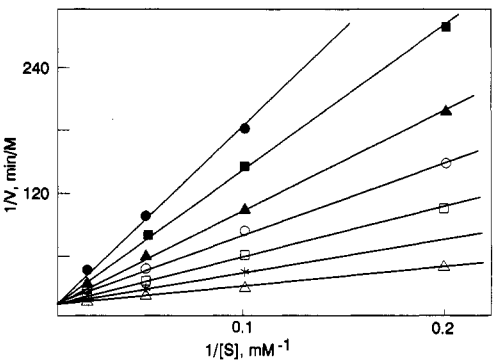

FIGURE 8: Lineweaver–Burk plots of methylcrotyl alcohol oxidation by χχ-ADH at the following millimolar pentanoate concentrations: (△) 50; (*) 20; (□) 10; (○) 5; (▲) 2.5; (■) 1; (●) none. The assays were carried out in 0.1 M glycine, 0.1 M Tris, 0.25 M NaCl, and 2.5 mM NAD$^+$ at pH 10.0.

Scheme I

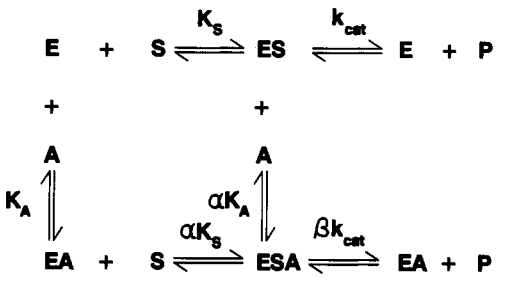

concentrations of cofactor (2.5 mM NAD$^+$).

The k_{cat}/K_m pH profile is qualitatively similar to that of ethanol (Wagner et al., 1984) with an activity maximum near pH 10.5 (Figure 7). Pentanoate does not change the bell shape of this curve but does shift the optimum down to near pH 10 as a result of an approximate 1 pH unit shift (11.2 to 10.1) of the upper ionization constant that determines the pH profile. However, the downshift of pK_2 does not explain the large increase of k_{cat}/K_m in the presence of pentanoate: the latter is due to the very large increase in the pH-independent k_{cat}/K_m constant (Figure 7) when pentanoate is added. In contrast, k_{cat} does not change significantly over the pH range investigated and is relatively insensitive to the presence of pentanoate.

Mechanism of Activation. Increasing concentrations of activator decrease the Michaelis constants for MCA (Figure 8) and pentanol (Table III) but do not markedly change k_{cat} values. This behavior can be analyzed in terms of nonessential activation according to Scheme I.

In Scheme I, E refers to the enzyme–NAD$^+$ complex, A to the activator, S to the alcohol substrate, and P to the products. The individual constants of Scheme I (Table IV)

Table IV: Kinetic Parameters for Scheme I[a]

alcohol	activator	K_m^{Alc} (mM)	K_A (mM)	α	β
MCA	pentanoate	15	28	0.072	0.70
pentanol	3-methyl-2-butenoate	28	110	0.16	2.1

[a] Data calculated from Figure 6 and Table III.

were obtained from secondary reciprocal plots of the slope of the Lineweaver–Burk plots and of the difference between the apparent Michaelis constant with and without activator as a function of activator concentration (Segel, 1975). These values clearly show that the major influence of the activator is to potentiate the binding of alcohol to the enzyme–cofactor binary complex. The β values are close to 1, but the α values are considerably less than 1, indicating that in the presence of activator the reaction pathway strongly tends to pass through the EA path (Scheme I) due to the considerably lowered apparent Michaelis constant (with a limit of αK_m).

Discussion

Class III ADH oxidizes ethanol and reduces acetaldehyde (Wagner et al., 1984; Deetz et al., 1984) but binds them so poorly that their K_m values cannot be determined even when ethanol is employed at concentrations up to 3 M. Indeed, the oxidation of any substrate by class III ADH examined thus far is less efficient with this enzyme than with any of the other human isozymes (Table II; Wagner et al., 1983, 1984). The recent discovery that rat $\chi\chi$-ADH is identical with glutathione-dependent formaldehyde dehydrogenase (Koivusalo et al., 1989) generates a renewed interest as to the physiological role of the enzyme and may give some insight into its mechanism. Indeed, human $\chi\chi$-ADH purified by the new HPLC procedure described here exhibits activity toward *S*-(hydroxymethyl)glutathione as well as other long-chain primary alcohols. In this respect, the activation of the oxidation of ethanol and longer alcohols by relatively large anions is another potential clue as to the origin of the enzymes's specificity.

The role of fatty acids in $\chi\chi$-ADH activity has been examined here with ethanol and other substrates. The rate of ethanol oxidation can be enhanced, primarily as a result of enhanced substrate binding, and is dependent to a degree on the size of the hydrocarbon component of the anionic activator. It thus becomes clear that the rate of ethanol oxidation catalyzed by $\chi\chi$-ADH is suboptimal and can be enhanced significantly by the presence of hydrophobic anions.

The phenomenon of $\chi\chi$-ADH activation by large anions, however, is not restricted to ethanol; the oxidation of other larger alcohols is also enhanced to a degree that jointly depends on the sizes of the substrate and activator. Thus, in general, long-chain acids activate short-chain alcohols; moderate-length acids (five carbons) are optimal in conjunction with moderately sized alcohols, but longer chain substrates (eight or more carbons) are not activated (Figure 3). The same applies to the reverse reaction. The reduction of aldehydes can be activated by hydrophobic anions, and methylcrotyl aldehyde reduction is activated by pentanoate, resulting in the largest enhancement observed, 30-fold.

The enhancement of $\chi\chi$-ADH-catalyzed methylcrotyl alcohol oxidation by pentanoate (Figure 8, Table IV) fits the nonessential activation mechanism (Scheme I). Several rationales to explain the kinetic results have been tested. The presence of pentanoate does not change the type of kinetic mechanism for methylcrotyl alcohol oxidation. Also, in the pH range from 9 to 11, no significant pK shift occurs on the E–NAD$^+$–S ternary complex (Figure 7, k_{cat} profile). For

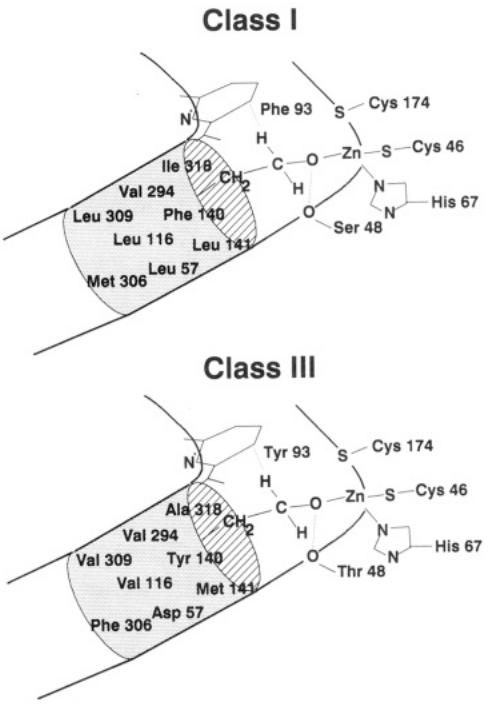

FIGURE 9: (Top) Schematic representation of the active site of horse liver ADH showing the hydrophobic "barrel" where long-chain substrates interact. (Bottom) The corresponding site in $\chi\chi$-ADH shows the maintenance of the hydrophobic region where activators likely interact. Adapted from Eklund and Brändén (1987).

E–NAD$^+$, there is a downshift of the upper ionization constant (Figure 7, k_{cat}/K_m profile), but such a shift should decrease the apparent ratio of kinetic constants. Hence, the observed increase arises from that of the k_{cat}/K_m value. It therefore appears that, according to Scheme I, the major source of activation lies in an enhanced binding of the substrate as quantitatively described in the values of α and β (Table IV). In this respect, results of chemical modification studies (in preparation) indicate that the activator anionic group most probably interacts with at least one arginine residue of $\chi\chi$-ADH. It may thus be inferred that binding of the activator induces a conformational change of the enzyme in such a way that the substrate interacts more strongly with the active site.

Although anions have been shown to activate different forms of ADH, the activation mechanism for class III ADH appears unique to this enzyme. For instance, binding of acetate to Arg-47 of horse EE ADH (His is the comparable residue in $\chi\chi$-ADH) increases ethanol oxidation by increasing the rate of reduced cofactor dissociation, the rate-limiting step of the reaction; larger anions inhibit the enzyme by binding to the zinc atom (Oldén & Pettersson, 1982). Similarly, bile acids have been shown to activate ethanol oxidation catalyzed by rat liver ADH (probably class I) (Hanozet et al., 1976); the bile acids change the kinetic mechanism (Hanozet et al., 1979) likely by binding to a specific lysine residue (Simonetta & Hanozet, 1980). Clearly, these effects differ from those observed with class III ADH.

On the basis of the crystallographic structure of horse EE ADH (Brändén et al., 1975) and on its significant homology to human class III ADH (Kaiser et al., 1988), the active site of the latter comprises a long hydrophobic region, referred to as a barrel (Eklund & Brändén, 1987), at the end of which the substrate hydroxyl or carbonyl group binds to the catalytic zinc atom. Modeling of the primary structure of $\chi\chi$-ADH to that of the horse enzyme indicates that there are extensive substitutions making the hydrophobic barrel of $\chi\chi$-ADH more hydrophilic (Figure 9). The catalytic zinc atom is not the

likely binding locus since such a mode of binding will result in inhibition as has been observed with human class I and the horse EE isozymes (Andersson et al., 1981). The inhibition of χχ-ADH observed with some large substrates at high activator concentrations suggests that direct binding to zinc is possible, however. Given a substrate of a certain length, there is an optimal size for the activator, above which the activation is progressively lost, indicating that a substrate and activator might compete with each other, perhaps in overlapping regions of the hydrophobic barrel. Thus, despite the multiple modes of binding to class III ADH available for hydrophobic anions, they appear to interact preferentially with a locus at least partially distinct from the substrate binding site to confer higher activity.

The involvement of hydrophobic anions appears to be a distinct and unique means to regulate the activity of class III ADH. The enzyme likely has an important function based on its pervasive presence in most tissues of many species, but, as yet, its exact physiological function is unknown. The degree of activation observed for ethanol oxidation thus far in vitro is not sufficient to suggest a role for χχ-ADH in ethanol metabolism. On the basis of the results presented here, a more likely natural substrate for the enzyme would be a compound bearing a primary alcohol or aldehyde, an anionic (carboxylic) function at a distance equivalent to about 8–10 carbons, and perhaps a nucleophilic group, sulfur, or a double bond which appears to provide highest k_{cat}/K_m values, adjacent to the hydroxyl. *S*-(Hydroxymethyl)glutathione meets these criteria as do several other alcohols. In the case of *S*-(hydroxymethyl)glutathione, it had previously been thought that the enzyme has a very high degree of specificity toward this particular hemithiol acetal. With the exception of homoglutathione, no other hemithiol acetals have been found to be substrates. However, those putative substrates which have been examined lack the presence of an anionic group 8–10 carbon atoms from the alcohol moiety, and thus the importance of anionic recognition as a component of this ADH's specificity has not been recognized. It is likely that, with the recognition of the anionic preference, new substrates will be discovered. In this regard, 20-hydroxyleukotriene B_4, a natural metabolite having most of these attributes, is an excellent substrate for human χχ-ADH (W. P. Dafeldecker, personal communication), and an enzyme having the characteristics for class III ADH has recently been isolated from human neutrophils following the activity toward this substrate (Gotoh et al., 1989).

References

Adinolfi, A., Adinolfi, M., & Hopkinson, D. A. (1984) *Ann. Hum. Genet. 48*, 1.

Andersson, P., Kvassman, J., Oldén, B., & Pettersson, G. (1981) *Eur. J. Biochem. 118*, 119.

Beisswenger, T. B., Holmquist, B., & Vallee, B. L. (1985) *Proc. Natl. Acad. Sci. U.S.A. 82*, 8369.

Brändén, C.-I., Jörnvall, H., Eklund, H., & Furugren, G. (1975) *Enzymes (3rd Ed.) 11*, 103.

Cleland, W. W. (1967) *Adv. Enzymol. Relat. Areas Mol. Biol. 29*, 1.

Dafeldecker, W. P., & Vallee, B. L. (1982) *J. Protein Chem. 1*, 59.

Dafeldecker, W. P., & Vallee, B. L. (1986) *Biochem. Biophys. Res. Commun. 143*, 1056.

Deetz, J. S., Luehr, C. A., & Vallee, B. L. (1984) *Biochemistry 23*, 6822.

Ditlow, C. D., Holmquist, B., Morelock, M., & Vallee, B. L. (1984) *Biochemistry 23*, 6363.

Eklund, H., & Brändén, C.-I. (1987) in *Biological Macromolecules and Assemblies* (Jurnak, F. A., & McPherson, A., Eds.) Vol. 3, pp 73–142, Wiley, New York.

Eklund H., Müller-Wille, P., Horjales, E., Futer, O., Holmquist, B., Vallee, B. L., Höög, J.-O., Kaiser, R., & Jörnvall, H. (1990) *Eur. J. Biochem. 193*, 303–310.

Gotoh, Y., Sumimoto, H., & Minakami, S. (1989) *Eur. J. Biochem. 179*, 315.

Hanozet, G. M., Simonetta, M., & Gerola, G. (1976) *FEBS Lett. 65*, 120.

Hanozet, G. M., Simonetta, M., Barisio, D., & Guerritore, A. (1979) *Arch. Biochem. Biophys. 196*, 46.

Jörnvall, H., Höög, J.-O., von Bahr-Lindström, H., & Vallee, B. L. (1987) *Proc. Natl. Acad. Sci. U.S.A. 84*, 2580.

Juliá, P., Parés, X., & Jörnvall, H. (1988) *Eur. J. Biochem. 172*, 73.

Kaiser, R., Holmquist, B., Hempel, J., Vallee, B. L., & Jörnvall, H. (1988) *Biochemistry 27*, 1132.

Kaiser, R., Holmquist, B., Vallee, B. L., & Jörnvall, H. (1989) *Biochemistry 28*, 8432.

Kaiser, R., Holmquist, B., Vallee, B. L., & Jörnvall, H. (1991) *FEBS Lett.* (in press).

Koivusalo, M., Baumann, M., & Uotila, L. (1989) *FEBS Lett. 257*, 105.

Laemmli, U. K., & Favre, M. (1973) *J. Mol. Biol. 80*, 575.

Lowry, O. H., Rosebrough, N. J., Farr, A. L., & Randall, R. J. (1951) *J. Biol. Chem. 193*, 265.

Oldén, B., & Pettersson, G. (1982) *Eur. J. Biochem. 125*, 311.

Parés, X., & Vallee, B. L. (1981) *Biochem. Biophys. Res. Commun. 98*, 122.

Segel, I. H. (1975) in *Enzyme Kinetics*, Wiley, New York.

Simonetta, M., & Hanozet, G. M. (1980) *Experentia 36*, 820.

Theorell, H., & Chance, B. (1951) *Acta Chem. Scand. 5*, 1127.

Uotila, L., & Koivusalo, M. (1974) *J. Biol. Chem. 249*, 7653.

Valkonen, K. H., & Goldman, D. (1988) *Electrophoresis 9*, 132.

Vallee, B. L., & Bazzone, T. J. (1983) *Curr. Top. Biol. Med. Res. 8*, 219.

Wagner, F. W., Burger, A. R., & Vallee, B. L. (1983) *Biochemistry 22*, 1857.

Wagner, F. W., Parés, X., Holmquist, B., & Vallee, B. L. (1984) *Biochemistry 23*, 2193.